

Single-Walled Carbon Nanotubes for a Strain-based Magnetometer

Stephanie A. Getty
Materials Engineering Branch, Code 541
NASA Goddard Space Flight Center
Greenbelt, USA
Stephanie.A.Getty@nasa.gov

Gunther Kletetschka
Department of Physics, IACS
Catholic University
Washington, USA
Gunther.Kletetschka@gssc.nasa.gov

Abstract— A design for a single-walled carbon nanotube (SWCNT) magnetometer will be presented. The operating principle exploits the sensitivity of SWCNT electrical properties to strain. The sensor design consists of a free-standing mat of SWCNTs that is mechanically coupled to a magnetically responsive, high aspect-ratio Fe component. During operation, torque on the Fe needle will transduce ambient magnetic field strength into an electronic signal. Preliminary results of precursor SWCNT material will be presented, including magnetic field- and temperature-dependence of electron transport measurements, and implications for magnetometer operation will be discussed.

Keywords—single-walled carbon nanotube; electromechanical; electron transport; magnetotransport; magnetometer

I. INTRODUCTION

Recent studies of isolated single-walled carbon nanotubes (SWCNTs) have demonstrated high sensitivity to only moderate levels of strain [1-3]. In one experimental verification, a SWCNT under manipulation with an atomic force microscope tip shows two orders of magnitude decrease in electrical conductance for a 14° out-of-plane deflection angle [1]. Proof of principle of a SWCNT film-based strain sensor has been demonstrated using commercially available SWCNTs [4], but improvements in performance are likely possible with the use of high-quality SWCNTs grown by chemical vapor deposition (CVD). In contrast, silicon-based MEMS devices exhibit only a few percent change in electrical conductance for comparable deflection angles. This advantage in sensitivity illustrates the promise of single-walled carbon nanotubes as a nanoelectromechanical material for use in a myriad of strain-based sensing applications.

One such application, a strain-based magnetometer, will be the focus herein. Magnetometers are integral to space and Earth science and are used in various applications, from magnetospheric study to spacecraft attitude control. The SWCNT-based alternative is projected to be lightweight, low-power, and of comparable sensitivity (nanotesla-range) to a conventional fluxgate magnetometer [5].

II. METHODOLOGY

The SWCNT magnetometer design consists of three major components: a free-standing mat of SWCNTs, a suspended large aspect-ratio Fe needle, and a set of electrodes. A schematic is shown in Figure 1. Primary drivers of this design are device reliability and structural robustness. In addition, the theoretical prediction that the strongest electromechanical response is associated with small band gap semiconducting SWCNTs [2] demands that an ensemble be used for reproducibility in fabrication.

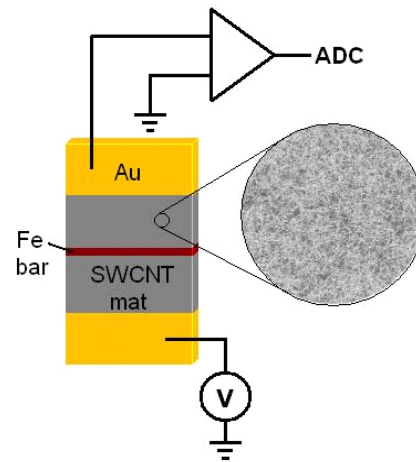


Figure 1. Schematic of SWCNT magnetometer design. The functional components consist of a mechanically free SWCNT basis, a magnetically responsive Fe bar, and electrodes to record an electromechanical response as the Fe needle is torqued in magnetic field.

Catalyst-assisted chemical vapor deposition (CVD) growth of SWCNTs was used to fabricate mats of nanotubes on a SiO_2/Si substrate. The substrate was first coated with Fe nanoparticles by exposure to a 20 mg $\text{Fe}(\text{NO}_3)_3$: 50 mL isopropanol solution for 30 s, followed by submersion in hexanes for 30 s. The substrate was then heated to 850°C for 5 minutes in flowing methane at 900 sccm (air), ethylene at 80 sccm (air), hydrogen at 580 sccm (air), and humid argon at 980 sccm (air) bubbled through deionized water [6-8]. A field-emission scanning electron micrograph is shown in Figure 2a,

where the bright islands are Fe catalyst, and the SWCNTs are shown as bright interconnected lines. Devices were fabricated by shadow evaporating 100 nm-thick Au electrodes spaced 54 microns apart. A field-emission scanning electron micrograph of one set of electrodes is shown in Figure 2b. The nanotubes are seen between the electrodes as interconnected dark lines in the center of the image. Preliminary studies of this SWCNT mat, labeled AB, and two similar devices, labeled CD and EF (not shown), are discussed below.

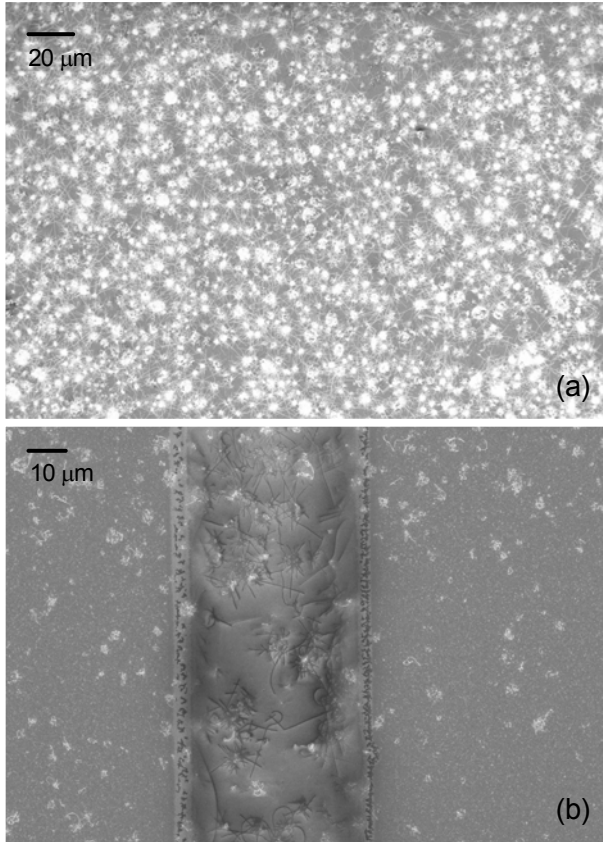


Figure 2. (a) Field-emission scanning electron micrograph of a CVD-grown SWCNT mat. (b) FESEM micrograph of device AB after shadow evaporation to define a set of Au electrodes.

Room temperature electrical characterization was performed using W micromanipulated probes (Signatone). Two-terminal current-voltage data were obtained by applying a dc voltage (Sorensen XT15-4 power supply) and measuring current using a Stanford Research Systems SR570 low-noise current pre-amplifier. Magnetic fields up to 0.4 T were applied transverse to the substrate with a GMW 5201 Projected Field Electromagnet, integrated with a homemade probe station. Low-temperature electronic measurements were performed using a homemade sample-in-vapor cryostat, fitted with a resistive heater and thermometry for temperature control.

III. RESULTS

Room temperature electron transport is shown in Figure 3 for devices AB, CD, and EF, where the device resistances are found to be 350 k Ω , 19 k Ω , and 47 k Ω , respectively. This dramatic variation in device resistance is likely due to differences in contact resistance and is not altogether unexpected. Because of the irreproducibility in quality of contacts, a working magnetometer is anticipated to require calibration prior to making quantitative field measurements.

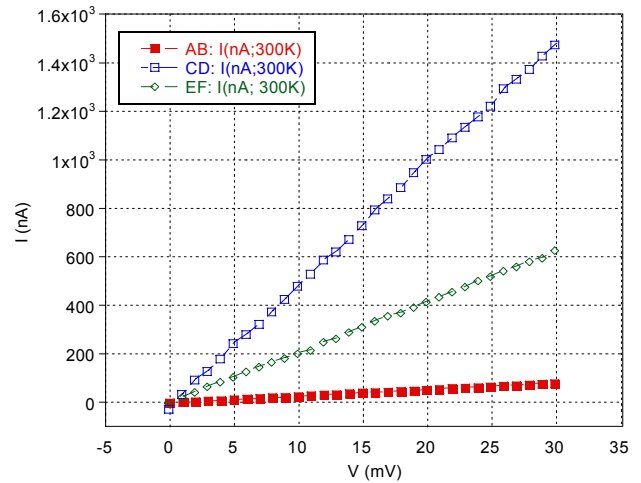


Figure 3. Current (nA) versus voltage (mV) in three SWCNT devices at room temperature. All devices are 54 microns in length and grown during a single CVD process. Large variations in device resistance are likely due to differences in contact resistance.

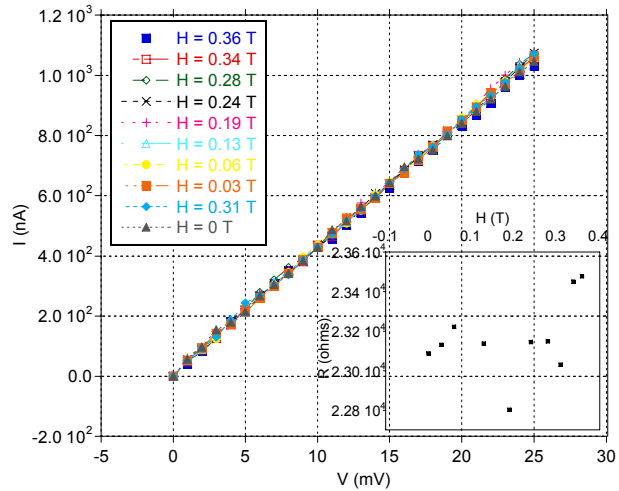


Figure 4. Current (nA) versus voltage (mV) for various values of applied magnetic field. (Inset) Resistance (Ω) versus magnetic field (T), showing no systematic field dependence.

A study of device resistance versus temperature, from 4.2 K to 300 K, was performed on devices AB and CD. Results are

shown in Figure 5. Resistance versus inverse temperature is shown in the inset.

A magnetic field up to 0.36 T was applied to device EF normal to the substrate plane and, therefore, transverse to the major axis of each SWCNT in the mat. In Figure 4, current-voltage curves are shown for variable magnetic field and exhibit no discernable dependence. Resistance versus magnetic field is shown in the inset.

IV. DISCUSSION OF MAGNETIC FIELD DEPENDENCE

To investigate the viability of using SWCNTs in a strain-based magnetometer the response of as-grown SWCNTs in variable magnetic field has been studied at room temperature. A ferromagnetic catalyst was used in the CVD growth process, and no attempts were made post-growth to remove the catalyst particles from the material. The presence of Fe nanoparticles in the film raises concerns that the SWCNT mat may exhibit an intrinsic magnetic field response, potentially attenuating the signal produced by an electromechanical operating mechanism.

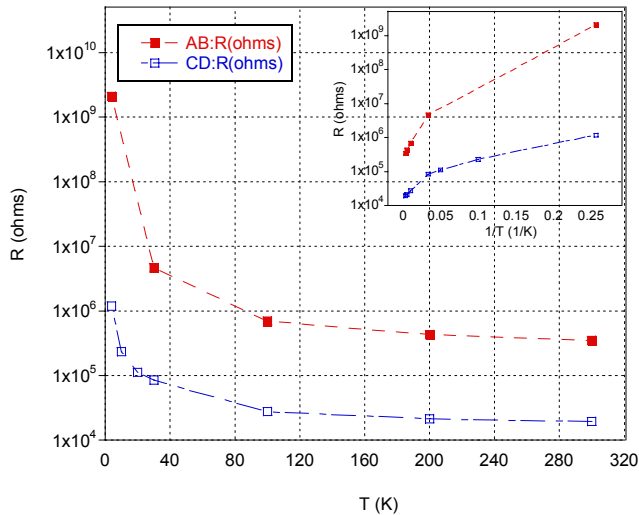


Figure 5. Resistance (Ω) versus Temperature (K) in devices AB and CD. (Inset) Resistance (Ω) on a logarithmic scale versus $1/\text{Temperature}$ ($1/\text{K}$) in two devices, AB and CD. A strong increase in device resistance is observed at low temperatures, with an apparent cross-over near 30 K. Effects intrinsic to semiconducting nanotubes and due to contact effects may be contributing to the observed temperature dependence.

The results shown in Figure 4 are encouraging in this respect. The electrical resistance shows no observed magnetic field dependence to 0.36 T, and these results were verified in cryogenic measurements. Although the targeted sensitivity of the magnetometer is nine orders of magnitude lower than this applied field, these results suggest that a large dynamic range will be possible.

It is interesting that the Fe nanoparticles do not induce a magnetic response in the SWCNT mat. We attribute this to prolonged handling in ambient conditions serving to oxidize the Fe material to a non-ferromagnetic form.

V. DISCUSSION OF TEMPERATURE DEPENDENCE

Temperature dependence of SWCNT mat resistance is an important parameter for two reasons: one practical and the other fundamental to predicting any limitations of this material as the basis of a strain sensor.

It is desirable that a magnetometer intended for space-based science be insensitive to thermal fluctuations, such that changes in the incidence of solar radiation do not dramatically affect operation. Devices AB and CD are found to approach a limiting value in resistance near room temperature. This behavior is interpreted to be satisfactory for high-temperature magnetometer operation. The rapid increase in resistance at low temperatures is too severe for reliable magnetic field measurement.

Quantitative mechanisms can be examined to describe the temperature dependence in an attempt to investigate the fundamental transport characteristics of these SWCNT devices. Intuitively, it is expected that the SWCNT mat will be dominated by the highest resistance in series and the lowest resistance in parallel. Assuming that both metallic and semiconducting tubes are present in each current path across the device length, then the constituent semiconducting nanotubes will dominate the intrinsic device. Contact resistance is likely also a contributor, however, in the form of a tunnel or Schottky barrier.

Standard theory of thermally activated transport in the presence of an energy barrier predicts that resistance follows an exponential dependence on temperature, as given in Equation 1 [9]:

$$R = R_0 \exp\left(\frac{\epsilon_g}{2k_B T}\right), \quad [1]$$

where R is the device resistance, ϵ_g is the energy gap, and T is the temperature. The slope of $\log R/R_0$ versus $1/T$, therefore, gives a measure of the energy gap. Quantitative analysis of the data shown in Figure 5 requires further detailed study, but qualitatively, the data are suggestive of two dominant energy scales in the high and low temperature limits. Furthermore, a larger energy gap can be extrapolated at high temperature in both devices and a lower energy gap at low temperatures, a trend that is physically sensible.

Temperature-dependent contact resistance may be a source of the observed behavior. For an imperfect barrier between the Au electrodes and the SWCNTs, phonon-assisted tunneling can constitute a considerable portion of the electron transport through the junction. Such thermally assisted processes can also give dramatic temperature dependence in the transport characteristics, and the temperature response in Figure 5 may represent thermally activated behavior governed by more than one characteristic energy scale. Further studies, including gate voltage dependence, are necessary to fully investigate these effects.

VI. CONCLUSIONS

We have demonstrated that the design for a strain-based magnetometer is compatible with experimental findings in

temperature and magnetic field studies of the SWCNT device basis. Despite the use of ferromagnetic material for a catalyst in the CVD growth process, a SWCNT mat does not exhibit discernable magnetic field dependence up to 0.36 T. Cryogenic studies of the SWCNT ensemble devices reveal that the material exhibits a strong low-temperature increase in resistance but is relatively insensitive to thermal variations at high temperature. These results suggest that SWCNT magnetometer operating conditions near room temperature or above will be most favorable. The strong cryogenic temperature dependence, however, may prove amenable to using SWCNT mats as temperature sensors or bolometric photon detectors in future device development.

ACKNOWLEDGMENT

S.G. would like to acknowledge the Summer Internship Program and Frank J. Wineland for contributions to SWCNT growth parameter characterization. This work was supported by the NASA GSFC Director's Discretionary Fund.

REFERENCES

- [1] T. Tombler, C. Zhou, L. Alexeyev, J. Kong, H. Dai, L. Liu, C. Jayanthi, M. Tang, and S. Y. Wu, *Nature* **405**, 769 (2000).
- [2] A. Maiti, A. Svizhenko, and M. P. Anantram, *Phys. Rev. Lett.* **88**, 126805 (2002).
- [3] J. Cao, Q. Wang, and H. Dai, *Phys. Rev. Lett.* **90**, 157601 (2003).
- [4] P. Dharap, Z. Li, S. Nagarajaiah, and E. V. Barrera, *Nanotechnology* **15**, 379 (2004).
- [5] For a review, see M. H. Acuna, *Rev. Sci. Instruments* **73**, 3717 (2002).
- [6] Hafner, J. H.; Cheung, C.-L.; Oosterkamp, T. H.; Lieber, C. M. *J. Phys. Chem. B* **105**, 743 (2001).
- [7] Kim, W.; Choi, H.-C.; Shim, M.; Li, Y.; Wang, D.; Dai, H. *Nano Lett.* **2**, 703 (2002).
- [8] K. Hata, D. N. Futaba, K. Mizuno, T. Namai, M. Yumura, S. Iijima, *Science* **306**, 1362 (2004).
- [9] N. F. Mott, *Metal-insulator Transitions*, Taylor and Francis (London, New York) 2000.